IMPERFECTION SENSITIVITY OF LAMINATED CYLINDRICAL SHELLS IN TORSION AND AXIAL COMPRESSION

G. J. Simitses+ and D. Shaw++
Georgia Institute of Technology
Atlanta, Georgia 30332

ICAS-84-3.5.1

I. Sheinman*
Technion-Israel Institute of Technology
Haif , Israel

Abstract

The imperfection sensitivity of thin cylindrical shells, made out of fiber reinforced composite material and subjected to either uniform axial compression or torsion, and the effects upon it of certain parameters are investigated. The sensitivity is established through plots of critical loads (limit point loads) versus imperfection amplitude. The larger the drop in critical load value with increasing amplitude, the greater the sensitivity. Results are presented for four- and six-ply laminates with simply supported boundaries and various stacking sequences. These sequences lead to symmetric, antisymmetric and asymmetric configurations with respect to the laminate midsurface. The material for all configurations is Boron/Epoxy. The parametric studies include primarily the effect of lamina stacking and length to radius ratio on the critical loads. Among the important findings one may list that (a) laminated cylindrical shells are more imperfection sensitive under axial compression than under torsion, (b) the imperfection sensitivity decreases as the length to radius ratio increases and (c) lamina stacking has a pronounced effect on the imperfection-sensitivity of the laminated shell.

I. Introduction

The circular cylindrical shell has been used extensively as a structural configuration especially in the aircraft and spacecraft industry. The constant demand for lightweight efficient structures has led the structural engineer to the use of various constructions (metallic with and without stiffeners, sandwich, laminated etc.), to more refined theoretical analyses, and to the field of structural optimization. Regardless of the construction, this configuration is not free of initial geometric imperfections. Moreover, in their service and function, cylindrical shells are often and usually subjected to destabilizing loads. Therefore, the aircraft structures engineer is interested in the stability analysis of these systems, in the presence of small initial geometric imperfections, especially for uniform axial compression and torsion.

Stability of thin circular cylindrical shells has received deserving attention from structural engineers, during the past seventy or so years. The multitude of theoretical and experimental studies, during this period, has tremendously enhanced our understanding of the buckling phenomenon and it has established that metallic thin cylindrical shells are extremely sensitive to initial geometric imperfections, especially when loaded axially. This is also true, to a lesser extend, for stiffened metallic cylindrical shells under axial compression. A fairly complete historical accounting of studies on the stability of axially loaded cylindrical shells with metallic construction (with and without stiffeners) is given in Ref. 1, and the cited references, therein. From this group, the attention of the interested reader is particularly directed towards the review articles of Hoff(2) and Hutchinson and Koiter(3). For this same construction (metallic), the studies of stability and imperfection sensitivity of cylindrical shells is smaller in number, when dealing with the load cases of torsion and pressure.

For the case of torsion a few references are cited, herein. These references deal primarily with the question of imperfection sensitivity, but if one adds to them their cited references, he has a fairly complete bibliography on the subject. Loo(4) and Nash(5) are among the first to report on the effect of small initial imperfections on the torsional critical load for simply supported(4) and clamped(5) isotropic cylindrical shells. Budiansky(6) treated the same problem by employing Koiter's(7) initial postbuckling theory. Sheinman and Simitses(8) by employing a nonlinear analysis predicted critical loads (limit point loads) for stiffened configurations under torsion and/or combined loading that includes torsion. In addition, one must cite the reported investigations of Hayashi(9), Becker(10), and Baruch, Singer and Weller(11).

Finally, there exist several references dealing with the case of external pressure, and a few for the case of combined loading. Although the paper deals with the cases of axial compression and torsion, some of the references related to pressure loading are cited herein, for the sake of completeness. Among these one must list the classic paper on closely stiffened (smeared technique) cylindrical shells by Baruch and Singer(12), the experimental results of Yamaki and Otomo(13) the analyses of Budiansky and Amazigo(14) and of Simitses et al(15).

With the advent of composite laminated shells, several investigations started appearing in the open literature which dealt with the subject of stability. In 1975, Tennyson(16) made a review of previous studies on the buckling of

+ Professor of Engineering Science and Mechanics, Associate Fellow of AIAA
++ Research Engineer
* Senior Lecturer in Civil Engineering, Member of AIAA

laminated cylinders. According to Tennyson's review, perhaps one of the earliest stability analyses of homogeneous orthotropic cylindrical shells was published by March et al.[17] in 1945. After that time, several theoretical analyses limited to orthotropic shells were performed by Schenell and Bruhl[18], Thielemann et al.[19], and Hess[21]. In these studies, simply supported end conditions were partially satisfied. The general linear theoretical solutions to anisotropic cylinders were presented by Cheng and Ho[21,22], Jones and Morgan[23], Jones and Hennemann[24] and Hirano[25]. Several papers were involved in the comparison of the efficiency and accuracy between Flugge's linear shell theory, which was employed by Cheng and Ho[21,22], and other shell theories (such as the work done by Tasi[26], Martin and Drew[27] whose theory was based on Donnell's equations, and the work of Chao[28], whose analysis was based on Timoshenko's buckling equations). Stiffened composite cylindrical shells have been analyzed by Jones[29], Terebushko[30] and Cheng and Card[31]. Theoretical analyses of the effect of initial geometric imperfections based on anisotropic shell theory, have been published for the loading cases of pure torsion[32] axial compression[33] and combined loads[34,35]. Moreover, several computer codes[36-49] (based on finite elements and/or differences) that deal with the analysis of stiffened shell configurations have been modified in order to account for laminated shell construction. These codes do serve their purpose, and that is that they are very good analytical tools. The purpose of the present paper is to assess the imperfection sensitivity of imperfect, laminated thin cylinders, subjected to uniform axial compression and torsion (individually applied). Moreover, parametric studies are performed in order to establish the effect of lamina stacking, and of the length to radius ratio on the critical conditions. As is well konwn[1], the imperfection sensitivity of systems (in this case thin cylindrical shells) has been established (a) through strict postbuckling analyses, (b) by employing Koiter's[7] theory, and (c) through nonlinear analyses of imperfect configurations[1,8,15] of known imperfection shape and amplitude. The methodology used in the present study is based on the last approach and is fully described in Ref. 48. All details concerning mathematical formulation, solution procedure and computer implementation can be found in Ref. 48. Only a brief description is included next, herein, for the sake of continuity and clarity.

II. Governing Equations

The geometry and reference frame, including sign convention, are shown on Fig. 1. The governing equations are derived for an orthogonally stiffened laminate, subjected to eccentric in-plane loads and uniform external pressure. The nonlinear governing equations (equilibrium) and related boundary conditions are derived from the principle of the stationary value of the total potential and they are based on Donnell-type nonlinear kinematic relations and linearly elastic material behavior. Moreover, the smeared technique[12] is used for the orthogonal stiffeners. Introduction of an Airy stress (resultant) function, F, defined below, leads to the identical satisfaction of the two in-plane equilibrium equations

$$N_{xx} = -N_{xx} + F_{,yy}; N_{yy} = F_{,xx}; N_{xy} = N_{xy} - F_{,xy} \quad (1)$$

where N_{xx} and N_{xy} are the applied in-plane loads. With this, the field equations are the third (transverse) equilibrium equation and the (in-plane) compatibility equation. Both of these, as well as the related boundary conditions, are expressed solely in terms of w and F, and their space-dependent deratives. These are:

(i) Equilibrium

$$\begin{aligned}
&b_{11}F_{,yyxx} + b_{21}F_{,xxxx} - b_{31}F_{,xxxy} + \\
&d_{11}w_{,xxxx} + d_{12}w_{,xxyy} + 2d_{13}w_{,xxxy} + \\
&2b_{13}F_{,xyyy} + 2b_{23}F_{,xxxy} - 2b_{33}F_{,xxyy} + \\
&2d_{31}w_{,xxxy} + 2d_{32}w_{,xyyy} + 4d_{33}w_{,xxyy} + \\
&b_{12}F_{,yyyy} + b_{22}F_{,xxyy} - b_{32}F_{,xyyy} + \\
&d_{21}w_{,xxyy} + d_{22}w_{,yyyy} + 2d_{23}w_{,xyyy} + \\
&\frac{1}{R}F_{,xx} + F_{,yy}(w_{,xx} + w^{o}_{,xx}) - \overline{N}_{xx}(w_{,xx} + w^{o}_{,xx}) + \\
&2\overline{N}_{xy}(w_{,xy} + w^{o}_{,xy}) - 2F_{,xy}(w_{,xy} + w^{o}_{,xy}) + \\
&F_{,xx}(w_{,yy} + w^{o}_{,yy}) + q = 0 \qquad (2)
\end{aligned}$$

(ii) Compatibility

$$\begin{aligned}
&a_{11}F_{,yyyy} + a_{12}F_{,xxyy} - a_{13}F_{,xyyy} + b_{11}w_{,xxyy} + \\
&b_{12}w_{,yyyy} + 2b_{13}w_{,xyyy} + a_{12}F_{,xxyy} + a_{22}F_{,xxxx} - \\
&a_{23}F_{,xxxx} - b_{21}w_{,xxxx} + b_{22}w_{,xxyy} + 2b_{23}w_{,xxxy} - \\
&a_{13}F_{,xyyy} - a_{23}F_{,xxxy} + a_{33}F_{,xxyy} - b_{31}w_{,xxxy} - \\
&b_{32}\,w_{,xyyy} - 2b_{33}\,w_{,xxyy} = w_{,xx}/R + w_{,xy}(w_{,xy} + \\
&2w^{o}_{,xy}) - w_{,xx}(w_{,yy} + 2w^{o}_{,yy})/2 - \\
&w_{,yy}(w_{,xx} + 2w^{o}_{,xx})/2 \qquad (3)
\end{aligned}$$

where the a_{ij}, b_{ij} and d_{ij} are the elements of the matrices that relate reference surface strains (ε^{o}_{ij}) and moment resultants M_{ij} to the stress resultants, N_{ij}, and the reference surface changes in curvature and torsion, κ_{ij} (for details see Ref. 48). In matrix form these relations are:

$$\{\varepsilon^{o}_{ij}\} = [a_{ij}]\{N_{ij}\} + [b_{ij}]\{\kappa_{ij}\} \qquad (4)$$

$$\{M_{ij}\} = [b_{ij}]^{T}\{N_{ij}\} + [d_{ij}]\{\kappa_{ij}\} \qquad (5)$$

where

$$[a_{ij}] = [\overline{A}_{ij}]^{-1}; \; [b_{ij}] = [\overline{A}_{ij}]^{-1}[\overline{B}_{ij}] \qquad (6)$$

and

$$[d_{ij}] = [\overline{B}_{ij}]\,[b_{ij}] - [\overline{D}_{ij}] \qquad (7)$$

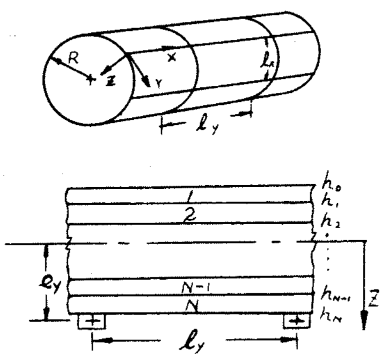

Fig. 1. Geometry and Sign Convention

Note that $[\bar{A}_{ij}]$, $[\bar{B}_{ij}]$ and $[\bar{D}_{ij}]$ are the matrices obtained from the usual lamination theory[49] and smeared technique for the stiffeners[1,12], when relating stress and moment resultants to reference surface strains and changes in curvature and torsion.

Moreover, the boundary conditions (at x = 0,L) for the case of simple supports, and all possible combinations of in-plane conditions, can be written as (same designation and notation are used, as in Hoff[2]),

$$
\begin{aligned}
&\text{SS-1} \quad w = 0;\ M_{xx} = \bar{M}_{xx};\ N_{xx} = -\bar{N}_{xx};\ N_{xy} = \bar{N}_{xy} \\
&\text{SS-2} \quad w = 0;\ M_{xx} = \bar{M}_{xx};\ u = \text{const.};\ N_{xy} = \bar{N}_{xy} \\
&\text{SS-3} \quad w = 0;\ M_{xx} = \bar{M}_{xx};\ N_{xx} = -\bar{N}_{xx};\ v = \text{const.} \\
&\text{SS-4} \quad w = 0;\ M_{xx} = M_{xx};\ u = \text{const.};\ v = \text{const.}
\end{aligned}
\tag{8}
$$

where $\bar{M}_{xx} = -\bar{E}\bar{N}_{xx}$, and $\bar{E}$ represents the eccentricity (distance from reference surface) of the applied stress resultant N_{xx} and is positive if in the positive z-direction.

The above boundary conditions may be written in terms of the dependent variables F and w. The final form of only SS-3 boundary conditions is shown herein for the sake of brevity.

<u>SS-3</u>: $w = 0;$

$$
\begin{aligned}
&b_{21}F_{,xx} + d_{11}w_{,xx} - b_{31}F_{,xy} = \bar{M}_{xx} + \\
&b_{11}\bar{N}_{xx} - b_{31}\bar{N}_{xy}\ ;\ F_{,yy} = 0; \\
&a_{22}F_{,xx} - a_{23}F_{,xy} + b_{21}w_{,xx} + 2b_{23}w_{,xy} = \\
&a_{12}\bar{N}_{xx} - a_{23}\bar{N}_{xy}
\end{aligned}
\tag{9}
$$

III. Solution Methodology

The solution methodology is presented, with detail, in Ref. 48. Only a brief description of it is presented below, for the sake of completeness.

The separated form, shown herein, for the dependent variables w and F is used to reduce the partial differential equations, Eqs (2) and (3), to ordinary differential equations.

$$
\begin{aligned}
&w(x, y) = A_o(x) + \sum_{i=1}^{k} [A_i(x) \cos\frac{iny}{R} + B_i(x) \sin\frac{iny}{R}] \\
&F(x,y) = C_o(x) + \sum_{i=1}^{2k} [C(x) \frac{iny}{R} + D_i(x) \sin\frac{iny}{R}]
\end{aligned}
\tag{10}
$$

The initial geometric imperfection $w^o(x,y)$ can also be presented in a similar form.

The above, is acomplished by first substituting the expressions for w,F, and w^o into the compatibility equation. Through trigonometric identities involving products, the compatibility equation reduces to a complete Fourier series from i = 0 to i = 2k [this justifies the need for using 2k in the expression for F, as opposed to k, see Eqs. (10)]. Use of orthogonality reduces the compatibility equation into (4k + 1) ordinary, nonlinear, differential equations.

Next, the Galerkin procedure is employed in connection with the equilibrium equation (in the circumferential direction only). This leads to the vanishing of (2k + 1) Galerkin integrals, which yields (2k + 1) additional nonlinear, ordinary, differential equations. Note from Eqs. (10) that the number of unknowns is (6k + 2), which equals the number of equations. Moreover, the boundary conditions, and the expressions for the total potential and average end shortening are also expressed in terms of the unknown functions of position x, shown in Eqs. (10).

Next, a generalization of Newton's method[50], applicable to differential equations, is used to reduce the nonlinear field equations to a sequence of linearized systems. The linearized (in the small increments) iteration equations are derived on the basis that a solution can be achieved by a small correction to an approximate solution.

Finally, the linearized set of differential equations is cast into a set of finite difference equations. These equations are solved by an algorithm[51], which is a modification of the one described in Ref. 52. A computer program has been written for generating numerical solutions.

IV. Geometries Used in the Study

The studies reported herein, include assessment of imperfection sensitivity and of the effect of lamina stacking on the critical conditions of four- and six-ply laminated cylinders under axial compression and torsion (individually applied). Moreover, the effect of L/R-ratios on critical loads is assessed for all geometries. In all of these studies, the load eccentricity is taken to be zero and the boundaries are classical simply supported (SS-3).

The configurations used in the studies represent variations of two symmetric (with respect to the midsurface) geometries for which experimental results are reported in Ref. 53. They consist of four-ply laminates, I-i and of six-ply laminates, II-i, both using different stacking sequences. For both groups five stacking sequences (i = 1,2,...5) are employed.

First, the common properties of the orthotropic laminae (Boron/Epoxy; AVCO 5505)[53] are:

$$E_{11} = 2.0690 \times 10^8 \text{ kN/m}^2 \ (30 \times 10^6 \text{ psi})$$
$$E_{22} = 0.1862 \times 10^8 \text{ kN/m}^2 \ (2.7 \times 10^6 \text{ psi}) \tag{11}$$
$$G_{12} = 0.0448 \times 10^8 \text{ kN/m}^2 \ (0.65 \times 10^6 \text{ psi}) \quad \nu_{12}=0.21$$

Furthermore,

$$R = 19.05 \text{ cm } (7.5 \text{ in.}) \tag{12a}$$

and the length, L, is varied so that

$$L/R = 1,3 \text{ and } 5 \tag{12b}$$

The ply thicknesses $(h_k - h_{k-1})$ and the total laminate thickness for each group are:

$$\text{I-i;}\ h_k-h_{k-1} = 0.013462 \text{ cm } (0.0053 \text{ in.}) \tag{13a}$$
$$h = 4(h_k-h_{k-1}) = 0.05385 \text{ cm. } (0.0212 \text{ in.})$$

and

$$\text{II-i;}\ h_k-h_{k-1} = 0.008975 \text{ cm } (0.003533 \text{ in.})$$
$$h = 6(h_k-h_{k-1}) = 0.05385 \text{ cm } (0.0212 \text{ in.}) \tag{13b}$$

Note that for both groups (I-i and II-i), the radius to thickness ratio is 353.77.

For each group, the five stacking combinations are denoted by I-i or II-i, i = 1,2,..5 and they correspond to

I-i: 45°/-45°/-45°/45°; I-2: 45°/-45°/45°/-45°;

I-3=-[I-2];I-4: 90°/60°/30°/0°;

I-5:0°/30°/60°/90° (14a)

II-1: 0°/45°/-45°/-45°/45°/0°

II-2: -45°/45°/-45°/45°/-45°/45°

II-3: -[II-2] (14b)

II-4: 90°/72°/54°/36°/18°/0°

II-5: 0°/18°/36°/54°/72°/90°

Where the first number denotes the orientation of the fibers (strong orthotropic direction) of the outermost ply with respect to the x-axis, and the last of the innermost.

Geometries I-1 and II-1 are symmetric with respect to the midsurface and identical to those employed in Ref. 53. Geometries I-2,3 and II-2,3 denote antisymmetric, regular (h_k-h_{k-1}= constant) angle-ply laminates. Finally, geometries, I-4,5 and II-4,5 are completely asymmetric with respect to the midsurface.

For each load case, different imperfection shapes are employed, which are:

(α) <u>for uniform axial compression</u>

(a) for geometries I-i (i = 1,2..5)

$$w^o(x,y) = \xi h \sin\frac{\pi x}{L} \cos\frac{ny}{R}$$

for geometries II-i (i= 1,2,..5) (15)

$$w^o(x,y) = \xi h \left(-\cos\frac{2\pi x}{L} + 0.1 \sin\frac{\pi x}{L} \cos\frac{ny}{R}\right) \tag{16}$$

Note that the first one, Eq. (15), denotes a symmetric shape, while the second one, Eq. (16), an (almost) axisymmetric shape.

(β) <u>for torsion</u>

(a) for L/R = 1

$$\text{I-i:}\quad w^o(x,y) = 0.6235\,\xi h\left[-\left(\sin\frac{\pi x}{L} - \frac{1}{3}\sin\frac{3\pi x}{L}\right)\cos\frac{ny}{R} + \left(\sin\frac{2\pi x}{L} - \frac{1}{2}\sin\frac{4\pi x}{L}\right)\sin\frac{ny}{R}\right] \tag{17a}$$

$$\text{II-i:}\quad w^o(x,y)= \xi h\left[-0.5831\left(\sin\frac{\pi x}{L} - \frac{1}{3}\sin\frac{3\pi x}{L}\right)\cos\frac{ny}{R} + 0.5479\left(\sin\frac{2\pi x}{L} - \frac{1}{2}\sin\frac{4\pi x}{L}\right)\sin\frac{ny}{R}\right] \tag{17b}$$

(b) for L/R = 2 and both groups

$$w^o(x,y) = \xi h\left[-0.5368\left(\sin\frac{\pi x}{L} - \frac{1}{3}\sin\frac{3\pi x}{L}\right)\cos\frac{ny}{R} + 0.6710\left(\sin\frac{2\pi x}{L} - \frac{1}{2}\sin\frac{4\pi x}{L}\right)\sin\frac{ny}{R}\right] \tag{18}$$

(c) for L/R = 5 and both groups

$$w^o(x,y) = \xi h\left[-0.417\left(\sin\frac{\pi x}{L} - \frac{1}{3}\sin\frac{3\pi x}{L}\right)\cos\frac{ny}{R} + 0.694\left(\sin\frac{2\pi x}{L} - \frac{1}{2}\sin\frac{4\pi x}{L}\right)\sin\frac{ny}{R} + 0.833\left(\frac{1}{3}\sin\frac{3\pi x}{L} - \frac{1}{5}\sin\frac{5\pi x}{L}\right)\cos\frac{ny}{R}\right] \tag{19}$$

For this load case (torsion), the imperfection shape is taken to be similar to the linear theory buckling mode[54]. These shapes, Eqs. (17)-(19), represent some average of the modes of the various configurations (the modes are very similar for all configurations).

V. Results and Discussion

The results for all configurations are presented both graphically and in tabular form. Each group, though, is discussed separately.

Table 1 presents critical loads (limit point loads-uniform axial compression) for geometries I-i and three values of L/R (1,2 and 5). The imperfection shape for this group is symmetric, Eq. (15), and the amplitude parameter is varied from a small number up to two ($w^{o}max/h = \xi$). These results are shown on Figs. 2-4. It is seen from these figures that for L/R = 1 and small values for ξ ($\xi < 0.75$), the weakest configuration corresponds to I-2,3 (regular antisymmetric angle-ply laminate), while the strongest configuration is the asymmetric I-5 (except for a very small range of extremely small ξ - values). But, as L/R increases, I-2,3 yield the weakest configurations for virtually all ξ-values. Moreover, for L/R > 2 the order of going from the weakest to the strongest configuration is I-2,3, I-1,I-4 and I-5. Note that asymmetric stacking may be compared to eccentric positioning of the orthogonal stiffeners in metallic shells.

TABLE 1. CRITICAL LOADS; UNIFORM AXIAL COMPRESSION (I-i GEOMETRIES)

Geometry	ξ	$\bar{N}^{\ell}_{xx}$ in lbs/in (wave No. at Limit Pt)		
		L/R = 1	L/R = 2	L/R = 5
I-1	0.05	-	145.6 (6)	-
	0.10	130.7 (9)	-	153.7 (4)
	0.50	118.9 (9)	136.0 (6)	147.7 (4)
	1.00	104.5 (9)	123.0 (6)	135.9 (4)
	2.00	67.1 (9)	98.3 (6)	121.0 (4)
I-2,3	0.05	-	138.8 (6)	-
	0.10	126.7 (9)	-	145.3 (4)
	0.50	115.1 (9)	130.0 (6)	140.2 (4)
	1.00	98.6 (9)	118.7 (6)	129.0 (4)
	2.00	61.3 (9)	92.2 (6)	111.4 (4)
I-4	0.01	-	243.1 (8)	-
	0.05	-	232.0 (8)	254.4 (5)
	0.10	189.9 (12)	-	-
	0.50	130.7 (11)	178.0 (8)	211.5 (5)
	1.00	86.8 (11)	137.2 (8)	187.7 (5)
	2.00	46.1 (10)	90.0 (8)	153.4 (5)
I-5	0.05	-	233.3 (8)	292.9 (5)
	0.10	183.2 (11)	-	-
	0.50	146.3 (11)	191.0 (8)	268.3 (5)
	1.00	97.5 (12)	150.0 (8)	239.0 (5)
	2.00	48.0 (11)	109.5 (8)	194.0 (5)

Symmetric Imperfection, Eq. (15).

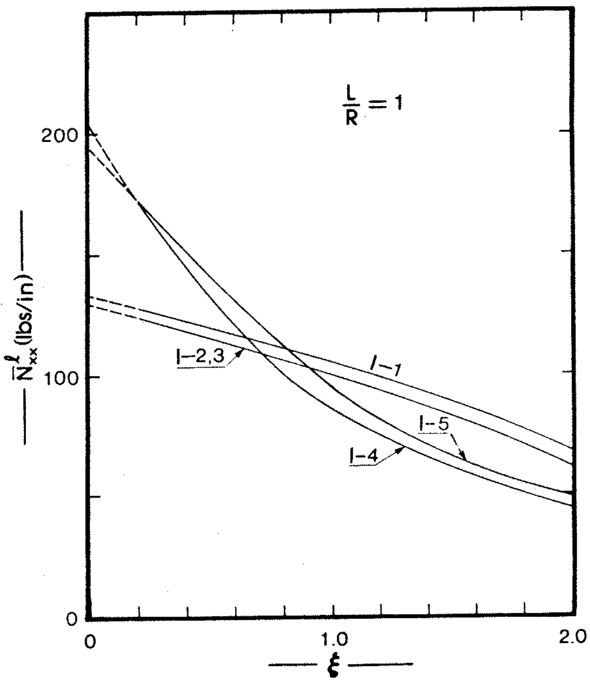

Fig. 2. Critical Conditions for I-i Geometries; Uniform Axial Compression; L/R = 1

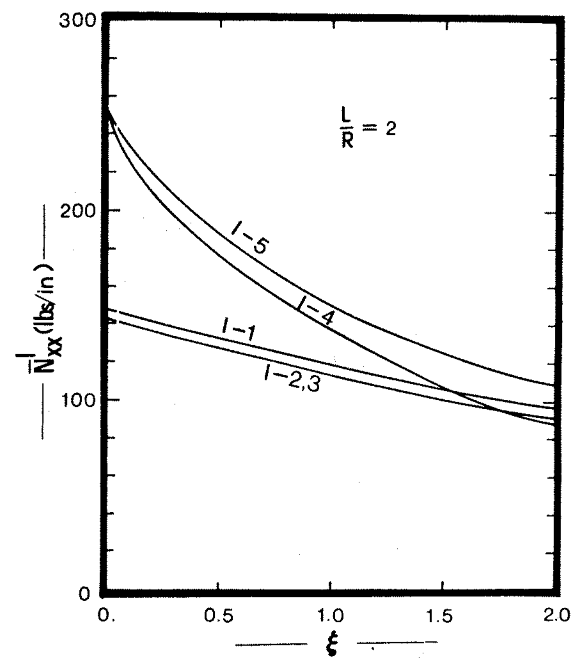

Fig. 3 Critical Conditions for I-i Geometries; Uniform Axial Compression; L/R = 2

Table 2 presents critical loads (uniform compresson) for geometries II-i. The results are similar to those for group I (geometries I-i) but with one exception; geometry II-1 is among the strong configurations, while I-1 is among the weak configurations, especially for higher L/R

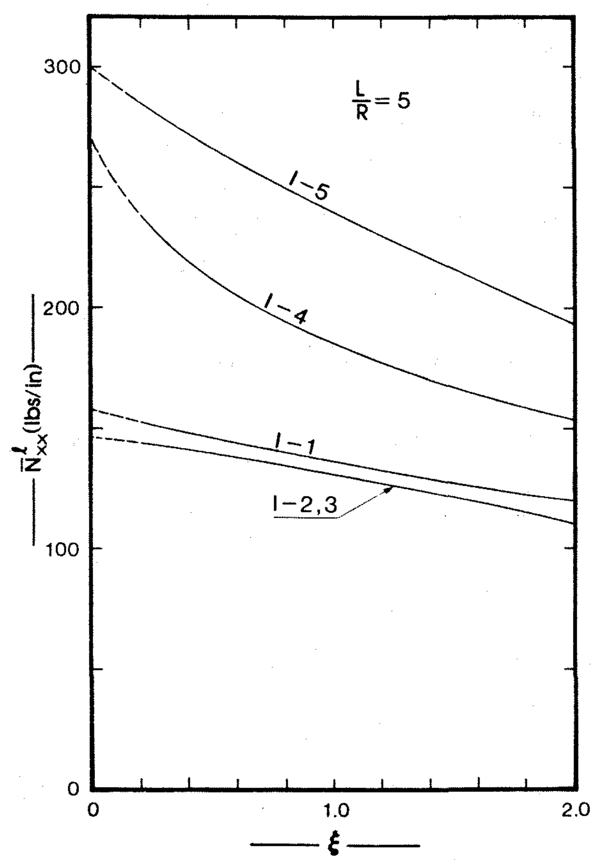

Fig. 4 Critical Conditions for I-i Geometries; Uniform Axial Compression; L/R = 5

ratios (see Figs. 5-7 and 2-4). The reason for this is that the II-1 geometry has 0^{o} plies on the outside and inside of the laminate, which increases its stiffness in the axial direction.

The results, for this group, are also presented graphically on Figs. 5-7. Fig. 5 contains results for L/R =1. No results are reported (limit points could not be found) for $\xi > 1.0$. This implies, that for this L/R value and $\xi > 1$ the load-deflection curve does not exhibit limit point instability, but only stable response. For L/R ≧ 2, the picture changed and limit points are found. Note from the three figures, Figs. 5-7, that as L/R increases the imperfection sensitivity of all configurations decreases (the curves do not fall as sharply as they do for L/R = 1).

It is worth noticing that for L/R ≦ 2, there are many crossings of the curves and it is not easy to identify the strongest or the weakest configuration (which is ξ-dependent). On the other hand, at L/R = 5, the strongest configuration is II-5 and the order of going from the strongest to the weakest is, II-5, II-1, II-4, II-2,3. As expected, the $\pm 45^{o}$ antisymmetric laminate is not the best layup for resisting axial compression. In this case also, it is observed that the imperfection sensitivity decreases with increasing (L/R)-values. Furthermore, in all cases, the weak configurations do not seem to be as sensitive as the stronger ones. The drop in value for the critical loads is very pronounced for geometries II-1, II-4, and II-5 (see Fig. 7) as ξ increases, while the drop is much more moderate for geometries II-2 & 3.

Table 2. CRITICAL LOADS; UNIFORM AXIAL COMPRESSION (II-i GEOMETRIES)

		$\bar{N}^{\ell}_{xx}$ in lbs/in.(wave No. at Limit Pt)		
Geometry	ξ	L/R = 1	L/R = 2	L/R = 5
II-1	0.10	231.7 (12	244.86 (8)	255.6 (5)
	0.50	120.9 (11)	171.3 (8)	219.4 (5)
	1.00	63.4 (10)	112.5 (8)	182.7 (5)
	2.00	-	58.4 (7)	128.2 (5)
II - 2,3	0.10	133.5 (9)	140.5 (6)	150.8 (4)
	0.50	120.7 (9)	134.6 (6)	147.8 (4)
	1.00	87.2 (9)	114.1 (6)	136.2 (4)
	2.00	44.7 (8)	72.6 (6)	111.4 (4)
II - 4	0.10	177.7 (10)	211.3 (8)	227.0 (5)
	0.50	101.7 (10)	157.0 (8)	199.3 (5)
	1.00	57.9 (10)	108.7 (7)	171.0 (5)
	2.00	-	56.8 (7)	128.8 (5)
II-5	0.10	173.5 (11)	199.5 (7)	275.0 (5)
	0.50	124.0 (10)	191.3 (7)	261.7 (5)
	1.00	66.7 (10)	139.0 (7)	227.9 (5)
	2.00		70.4 (7)	168.4 (5)

Axisymmetric Imperfection, Eq. (16).

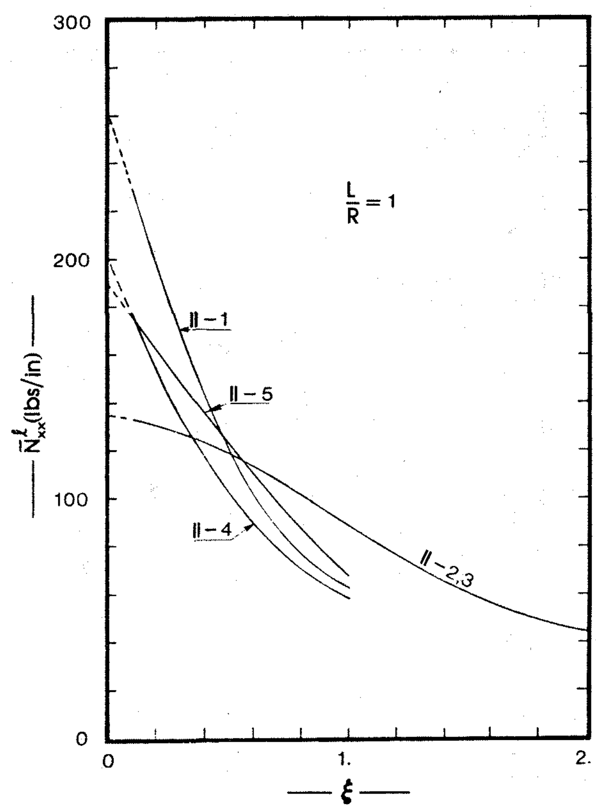

Fig. 5. Critical Conditions for II-i Geometries; Uniform Axial Compression; L/R = 1

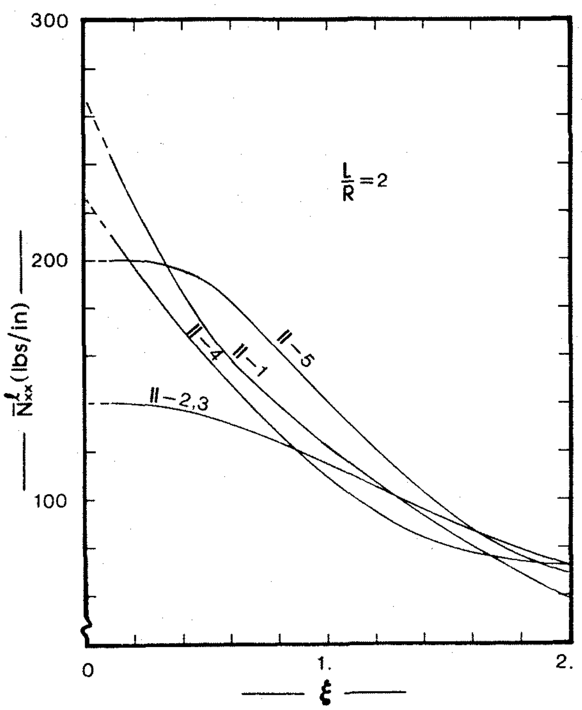

Fig. 6 Critical Conditions for II-i Geometries; Uniform Axial Compression; L/R = 2.

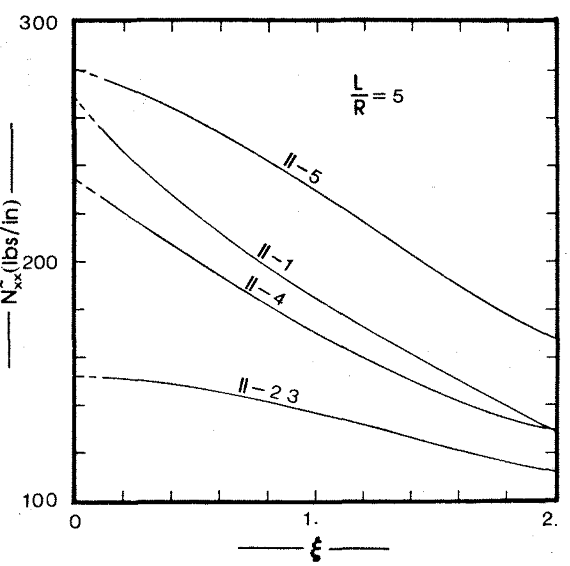

Fig. 7 Critical Conditions for II-i Geometries; Uniform Axial Compression; L/R = 5

Table 3 presents critical loads for geometries I-i subjected to torsion. The results are also presented graphically on Figs. 8-10. The reader is reminded that the imperfection shape for this load case is similar to the linear theory eigenmode (see Ref. 54) and is L/R-dependent. Regardless of the shape, the imperfection parameter, ξ, is equal to w_{max}/h. For all L/R values, the I-1 geometry seems to be the weakest one. On the other hand, geometry I-5 yields the strongest configuration. For L/R = 1 the I-2,3 configurations seem strong, but as L/R increases they become weaker by comparison to the asymmetric configurations. If torsion were to be reversed the strength of the I-2,3, configurations would remain unchanged (the role of I-2 and I-3 would be interchanged), while the asymmetric configurations could change for the worse. The reason for this expectation is that for positive torsion, tension is expected along a direction making a positive angle with x-axis (for isotropic construction it would have been ≈ 45^{o}). The fibers are placed from 0^{o} to 90 or from 90^{o} to 0^{o} in the various layers of I-5 and I-4. Thus, the tensile unidirectional strength of the fibers is utilized. If the torsion is reversed, these same fibers would tend to be in compression and this would imply that I-4 and I-5 are weaker for negative torsion than for positive torsion. Of course no mention is made of the effect of the (negative torsion) imperfection shape. This could be a totally separate study. Along these lines, note that the I-1 geometry (see Ref. 54) is stronger when loaded in the negative direction than in the positive direction, provided that the imperfection shape is similar to the positive torsion buckling mode.

Table 3. CRITICAL LOADS; TORSION (I - i GEOMETRIES)

Geometry	ξ	$\bar{N}_{xy}^{\ell}$ in lbs/in(wave No. at Limit Pt.)		
		L/R = 1	L/R = 2	L/R = 5
I-1	0.1	55.34 (15)	35.32 (11)	21.00 (7)
	0.5	45.36 (15)	31.57 (11)	19.43 (7)
	1.0	43.62 (15)	28.32 (1)	18.01 (7)
I-2	0.1	78.90 (13)	46.4 (9)	24.91 (6)
	0.3	73.16 (13)	-	-
	0.5	66.36 (13)	41.81 (9)	23.15 (6)
	1.0	-	37.89 (9)	21.57 (6)
I-3	0.1	79.34 (13)	46.36 (9)	24.84 (5)
	0.3	73.41 (13)	-	-
	0.5	66.50 (13)	41.84 (9)	23.08 (6)
	1.0	-	37.96 (9)	21.52 (6)
I-5	0.1	56.69 (16)	44.18 (12)	29.81 (8)
	0.5	45.91 (15)	38.75 (12)	27.16 (8)
	1.0	39.51 (14)	34.22 (12)	24.74 (8)
I-5	0.1	84.83 (16)	66.49 (12)	42.91 (8)
	0.5	64.20 (16)	56.91 (12)	38.50 (8)
	1.0	46.79 (15)	48.72 (12)	34.27 (8)

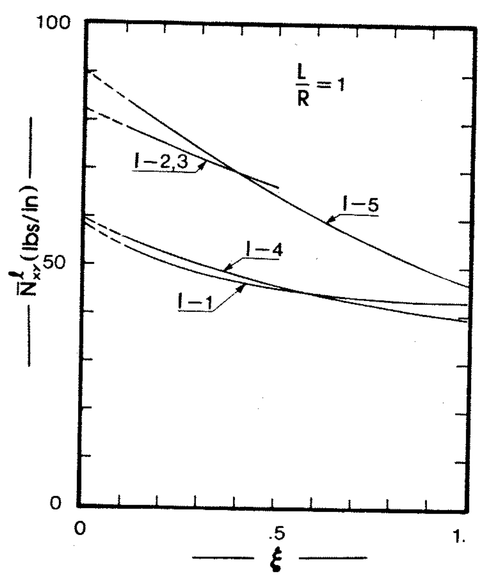

Fig. 8 Critical Conditions for I-i Geometries; Torsion; L/R = 1

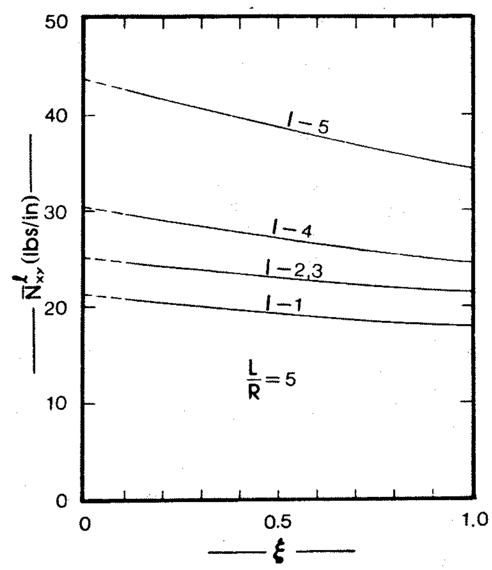

Fig. 10 Critical Conditions for I-i Geometries; Torsion; L/R = 5.

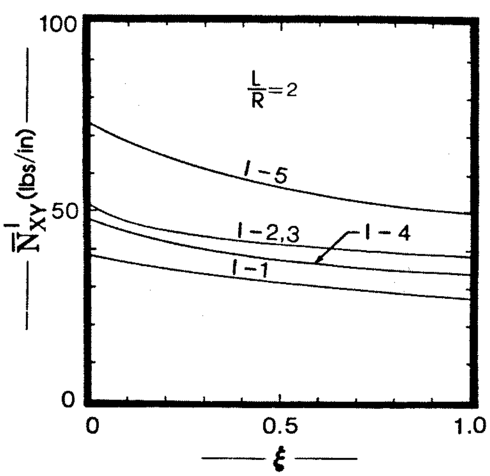

Fig. 9 Critical Conditions for I-i Geometries; Torsion; L/R = 2.

Table 4 presents critical torques for geometries II-i. The results are also presented graphically on Figs. 11-13. The conclusions are very similar to those for geometries I-i. There is one important observation, though, derived from the comparison of the two groups. Since both groups have the same total thickness (0.0212 in.) and radius (7.5 in.) use of more layers (from four to six) increases the load carrying capacity for the antisymmetric configurations (II-2,3 versus I-2,3), but it decreases it for the asymmetric configuration II-5 (it can even be said for II-4). The comparison between II-1 and I-1 is not valid, since II-1 contains two 0^{o}-plies (outer and inner), while I-1 has no such plies.

When the curves (see Fig. 8 and 11) terminate at $\xi = 0.5$, it means that no limit point could be found for higher ξ-values.

Moreover, it is seen from the generated data that (a) both groups are not as sensitive to initial geometric imperfection, when loaded in torsion, as they are for the case of axial compression, and (b) the imperfection sensitivity decreases (for this load case also) as the (L/R)-value increases.

Finally, experimental results are reported in Ref. 53, for geometry I-1, L/R = 2, and simply supported boundaries. The comparison between theoretical and experimental values can only be qualitative, for both load cases. Ref. 53 does not provide information concerning the imperfection shape and amplitude. The experimental results are:

I-1 (L/R = 2): $N_{xx_{cr}}$ = 105 lbs/in; $N_{xy_{cr}}$ = 26.5/in

The theoretical predictions can be found, graphically, in Figs. 3 and 9.

TABLE 4. CRITICAL LOADS: TORSION (II-i GEOMETRIES)

Geometry	ξ	$\bar{N}^{\ell}_{xy}$ in lbs/in (wave No. at Limit Pt) L/R = 1	L/R = 2	L/R = 5
II-1	0.1	53.54 (18)	38.49 (13)	25.50 (9)
	0.5	43.49 (17)	31.74 (13)	23.10 (9)
	1.0	40.15 (17)	27.17 (13)	20.92 (9)
II-2	0.1	82.46 (14)	48.25 (9)	26.17 (6)
	0.3	73.194(13)	-	-
	0.4	69.76 (12)	-	-
	0.5	-	42.43 (9)	24.50 (6)
	1.0	-	37.31 (9)	23.00 (6)
II-3	0.1	82.12 (13)	48.25 (9)	26.22 (6)
	0.3	73.07 (13)	-	-
	0.4	69.69 (13)	-	-
	0.5	-	42.45 (9)	24.55 (6)
	1.0	-	37.40 (9)	23.06 (6)
II-4	0.1	57.13 (16)	44.11 (12)	29.69 (8)
	0.5	44.23 (15)	37.73 (12)	27.36 (8)
	1.0	37.46 (15)	32.54 (11)	25.29 (8)
II-5	0.1	81.19 (16)	63.61 (13)	41.96 (8)
	0.5	56.42 (16)	52.33 (12)	38.10 (8)
	1.0	42.23 (14)	41.38 (13)	34.51 (8)

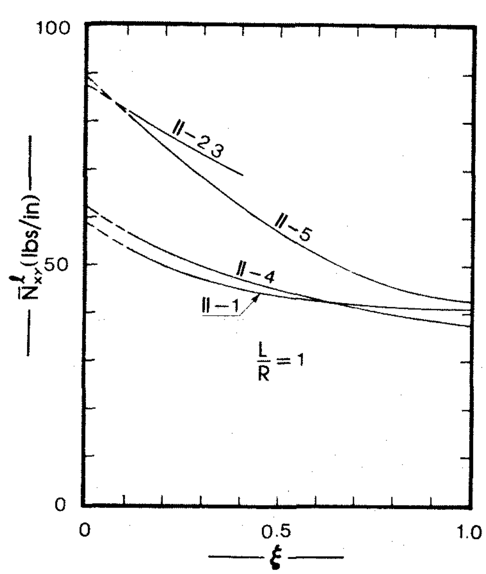

Fig. 11 Critical Conditions for II-i Geometries; Torsion; L/R = 1.

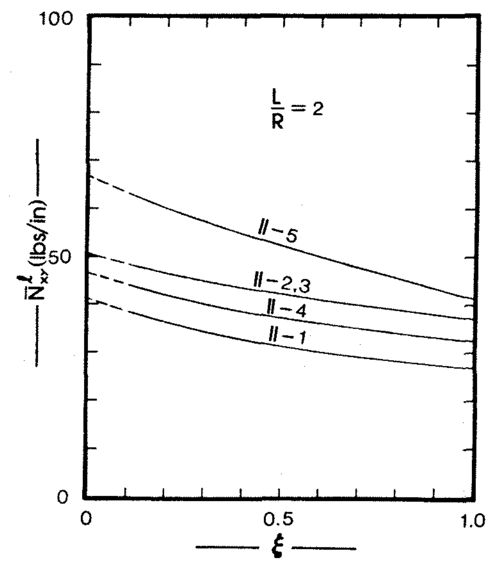

Fig. 12 Critical Conditions for II-i Geometries; Torsion; L/R = 2.

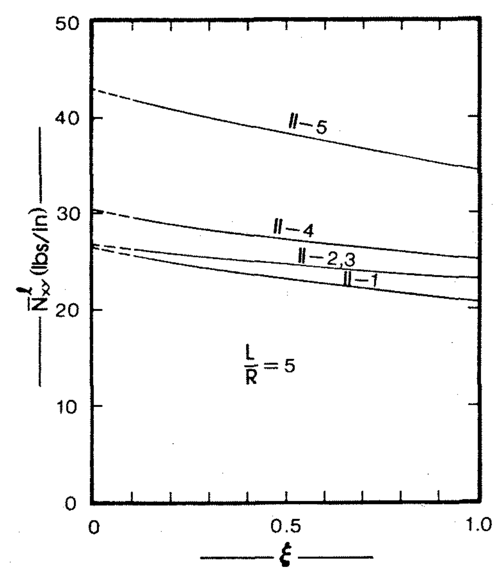

Fig. 13 Critical Conditions for II=i Geometries; Torsion; L/R = 5.

VI. Conclusions

A number of important conclusions can be drawn from the obtained results. Recognizing, though, that the employed configurations cannot possibly cover all values and variations for the geometric parameters (L/R, R/h ratios, imperfection shapes, etc), the structural parameters (material properties, numerous lay-ups, number of plies etc) and boundary conditions, then these conclusions should be considered only as observations and not necessarily as universal, in applicability.

Among the the most important observtion one may list the following:

(1) Under axial compression, some laminated geometries can be as sensitive to initial geometric imperfections as isotropic geometries are (very sensitive). On the other hand, some are not as sensitive.

(2) Under torsion, laminated geometries are less sensitive to geometric imperfections than under compression. This is also true for isotropic geometries.

(3) Regardless of the load case, the imperfection sensitivity of the cylindrical shell decreases with increasing (L/R)-values.

(4) Lamina stacking (symmetric, antisymmetric, asymmetric) does affect the critical loads. The stronger geometries are more sensitive to initial geometric imperfections than the weaker ones. This is true for both load cases.

References

1. Simitses, G. J., and Sheinman, I., "Buckling and Postbuckling of Imperfect Cylindrical Shells under Axial Compression" Computers and Structures, Vol. 17, No. 2, 1983, pp 277-285.
2. Hoff, N. J., "The Perplexing Behavior of Thin Circular Cylindrical Shells in Axial Compression" Israel Journal of Technology, Vol. 4 No. 1, 1966, pp 1-28.
3. Hutchinson, J. W., and Koiter, W. T., "Postbuckling Theory" Applied Mechanics Reviews, Vol. 12, 1970, pp 1353-1366.
4. Loo, T.T. "Effects of Large Deflections and Imperfections of the Elastic Buckling of Cylinders under Torsion and Axial Compression", Proceedings of the second U.S. National Congress of Applied Mechanics, 1954, pp 345-375.
5. Nash, W. A., "Buckling of Initially Imperfect Cylindrical Shells Subjected to Torsion ", Journal of Applied Mechanics, Vol. 24, 1957, pp 125-130.
6. Budiansky, B., "Post-Buckling Behavior of Cylinders in Torsion", in Theory of Thin Shells, edited by F.I. Niordson (IUTAM - sponsored Symposium, Copenhagen, 1967), Springer-Verlag, Berlin, 1969.
7. Koiter, W. T. "On the Stability of Elastic Equilibrium" (in Dutch) Thesis, Delft, Amsterdam 1945; English Translation NASA TT-F-10833, 1967.
8. Sheinman, I., and Simitses, G. J., "Buckling of Imperfect Stiffened Cylinders under Destabilizing Loads including Torsion", AIAA Journal, Vol. 15, No. 12, 1977, pp. 1699-1703.
9. Hayashi, T., Torsional Buckling of Orthogonal-Anisotropic Cylinders, Coronax, Japan, 1952.
10. Becker, H., "General Instability of Stiffened Cylinders" NACA TN 4237, Washington D.C., 1958.
11. Baruch, M., Singer, J., and Weller, T., "Effect of Eccentricity of Stiffeners on the General Instability of Cylindrical Shells under Torsion" Israel Journal of Technology, Vol. 4, No. 1, 1966, pp 114-154.
12. Baruch, M., and Singer, J. "Effect of Eccentricity of Stiffeners on the General Instability of Stiffened Cylindrical Shells under Hydrostatic Pressure" Journal of the Mechanical Engineering Sciences, Vol. 5, No. 1, 1963, pp 23-27.
13. Yamaki N., and Otomo, K., "Experiments on the Postbuckling Behavior of Circular Cylindrical Shells under Hydrostatic Pressure" Experimental Mechanics, July 1973, pp. 299-304.
14. Budiansky, B., and Amazigo, J.C., "Initial Postbuckling Behavior of Cylindrical Shells under External Pressure" Journal of Mathematics Physics, Vol. 47, 1968, pp 223-235.
15. Simitses, G.J., Sheinman, I., and Giri, J. "Nonlinear Stability Analysis of Pressure-Loaded Imperfect Stiffened Cylinders", Journal of Ship Research, Vol. 23, No. 2, June 1979 pp. 123-126.
16. Tennyson, R. C., "Buckling of Laminated Composite Cylinders: a Review," Composites, Vol. 1, 1975, pp 17-24.
17. March, H. W. et al. "Buckling of Thin-Walled Plywood Cylinders in Torsion," Forest Products Lab., Madison, Wisc. Report 1529, June, 1945.
18. Schenell, W. and Bruhl, C. "Die Langsgedruckte Orthotrope Kreiszylinder-schale bei Innendruck," Zeitschrift Flugwiss, Vol. 7, 1959.
19. Thielemann, W. F., Schenell, W., and Fischer, G., "Buckling and Postbuckling Behavior of Orthotropic Circular Cylindrical Shells Subjected to Combined Axial and Internal Pressure," Zeitschrift Flugwiss, Vol. 8, 1960.
20. Hess, T. E., "Stability of Orthotropic Cylindrical Shells under Combined Loading," J. American Rocket Society, Vol. 31, No. 2 1961, pp 237-241.
21. Cheng, S., and Ho. B. P. C., "Stability of Heterogeneous Aeolotropic Cylindrical Shells Under Shells Under Combined Loading", AIAA Journal, Vol. 1, No. 4, April, 1963, pp 892-898.
22. Ho, B. P. C., and Cheng, S. "Some Problems in Stability of Heterogeneous Aeolotropic Cylinrical Shells Under Combined Loading", AIAA Journal, Vol. 1, No. 7, July 1963, pp 1603-1607.
23. Jones, R. M., and Hennemann, J. C. F., "Effect of Prebuckling Deformations on Buckling of Laminate Composite Circular Shells," Proceedings of AIAA 19th Structures, Structural Dynamics and Material Conference, Bethesda, MD., April 1978.
24. Jones, R. M., and Morgan, H.S., "Buckling and Vibration of Cross-Ply Laminated Circular Cylindrical Shell", AIAA Journal, Vol. 13, No. 5, 1975, pp 664-671.

25. Hirano, Y., "Buckling of Angle-Ply Laminated Circular Cylindrical Shells", Journal of Applied Mechanics, Vol. 46, No. 1, 1979, pp 233-234.
26. Tasi, J., "Effect of Heterogeneity on the Stability of Composite Cylindrical Shells Under Axial Compression", AIAA Journal, Vol. 4, No. 6, June 1966, pp 1058-1062.
27. Martin, R. E., and Drew, D. D., "A Batdorf Type Modified Equation for the Stability Analysis of Anisotropic Cylindrical Shells," Texas A & M University, Tech. Report No. 10, March 1969.
28. Chao, T. L., "Minimum Weight Design of Stiffened Fiber Composite Cylinders," USAF, WPAFB Tech. Report AFML-TR-69-251, Sept. 1969.
29. Jones, R. M., "Buckling of Circular Cylindrical Shells With Multiple Orthotropic Layers and Eccentric Stiffeners" AIAA Journal, Vol. 6, No. 12, Dec. 1968, pp 2301-2305.
30. Terebushko, O.I., "Stability of Stiffened and Anisotropic Shells, "Transactions of 7th All-Union Conference on Theory of Plates and Shells, Dnepropetrovsk, Ukranian SSR, Sept. 1969.
31. Chang, L.K., and Card, M.F., "Thermal Buckling Analysis for Stiffened Orthotropic Cylindrical Shells," NASA TN-D6332, 1971.
32. Chehill, D.S. and Cheng, S. "Elastic Buckling of Composite Cylindrical Shells Under Torsion", Journal of Spacecraft and Rocketts, Vol. 5, No. 8, 1968, pp 973-978.
33. Tennyson, R. C., and Muggeridge, D. B., "Buckling of Laminated Anisotropic Imperfect Circular Cylinder Under Axial Compression," Journal of Spacecraft and Rockets, Vol. 10, No. 2, 1973, pp 143-148.
34. Booton, M., and Tennyson, R. C., "Buckling of Imperfect Anisotropic Circular Cylinders Under Combined Loading." AIAA Journal, Vol. 17, No. 3, 1979, pp 278-287.
35. Herakovich, C. "Theoretical-Experimental Correlation for Buckling of Composite Cylinders Under Combined Loads," NASA CR-157359, July 1978.
36. Tripp, L. L., Tamekuni, M., and Viswanathan, A. V., "User's Manual BUCLASP2: A Computer Program for Instability Analysis of Biaxially Loaded Composite Stiffened Panels and Other Structures," NASA CR-112, 226, 1973 (prepared by the Boeing Co. for Langley Research Center) [BUCLASP 2].
37. Wittrick, W. H., and Williams, F. W., "Buckling and Vibration of Anisotropic or Isotropic Plate Assemblies Under Combined Loadings," International Journal of Mechanical Sciences, Vol. 16, No. 4, 1974, pp. 209-239 [VIPASA].
38. Bushnell, D., "Stress Stability and Vibration of Complex Shells of Revolution. Analysis and User's Manual for BOSOR 3", Lockheed Missiles and Space Company Report N-5J-69-1, Sept. 1969, Palo Alto, California. [BOSOR 3].
39. Stanton, E. L., and McGovern, D. J., "The Application of Gradient Minimization Methods and Higher Order Discrete Elements to Shell Buckling and Vibration Eigen-value Problems," McDonnell-Douglas Astronautics Paper WD 1406, Sept. 1970 [DEBACUL].
40. Haisler, W. E., Stricklin, J. A., and Von Riesemann, W. A., "DYNAPLAS- A Finite Elemlent Program for the Dynamic Elastic-Plastic Analysis of Stiffened Shells of Revolution," TEES RPT-72-27, Department of Aerospace Engineering, Texas A & M University, College Station, Texas, December 1972. [DYNAPLAS].
41. Zudans, Z., "Input Map and User's Guide for the FELAP 8 Computer Program," Franklin Institute Research Laboratories, Jan. 1971 (Proprietry Document) [FELAP 8].
42. Huffington, N. J., Jr., "Large Deflection Elasto-Plastic Response of Shell Structures," Ballistic Research Laboratories BRL R 1515, Aberdeen Proving Grounds, Maryland, Nov. 1970 [REPSIL].
43. Anderson, J. S., Fulton, R. E., Heard, W. L., Jr., and Walz, I.E., "Stress Buckling and Vibration Analysis of Shells Revolution", Computers and Structures, Vol. 1, 1971, pp. 157-192 [SALORS].
44. Ball, R. E., "A Program for the Nonlinear Static and Dynamic Analysis of Arbitrarily Loaded Shells of Revolution," Computers and Structures, Vol. 2, 1972, pp. 141-162 [SATANS].
45. Prince, N., "SHELL-3D-The Structural Analysis of Arbitrary Three-Dimensional Thin Shells, Part I: Analytical Development and Part II: Program User's Manual for SHELL 9," Gulf General Atomic, Inc., Report GA-10130, July 1970 [SHELL 9].
46. Almroth, B.O. et al. "Collapse Analysis for Shells of General Shape; Volume II. - User's Manual for the STAGS -A. Computer Code". Technical Report AFDL-TL 71-8, Air Force Flight Dynamics Laboratory, Wright-Patterson AF Base, Ohio, 1973. [STAGS].
47. Hartung, F. G., "An Assessment of Current Capability for Computer Analysis of Shell Structures," Technical Report AFFDL-TR-71-54, Air Force Flight Dynamics Laboratory, Wright-Patterson AF Base, Ohio, 1971.
48. Sheinman, I., Shaw, D., and Simitses, G. J., "Nonlinear Analysis of Axially-Loaded Laminated Cylindrical Shells", Computers and Structures, Vol. 16, No. 1-4, 1983, pp.131-137.
49. Jones, R. M., Mechanics of Composite Materials, McGraw-Hill Book Co., New York, 1975.
50. Thurston, G. A., "Newton's Method Applied to Problems in Nonlinear Mechanics", J. Appl. Mech., Vol. 32, No. 2, (1965), p. 383.
51. Sheinman, I., and Simitses, G. J., "A Modification of Potter's Method for Diagonal Matrices with Common Unknown", Computers and Structures, Vol. 18, No. 2 (1984) pp. 273-275.
52. Tene, Y., Epstein, M., and Sheinman, I., "A Generalization of Potter's Method", Computers and Structures, Vol. 4, (1974) pp. 1099-1102.
53. Wilkins, D. J. and Love, T. S., "Combined Compression-Torsion Buckling Tests of Laminated Composite Cylindrical Shells", Proceedings of AIAA/ASME/SAE 15th Structures, Structurall Dynamics and Materials Conference, Las Vegas, Nevada, April 1974, AIAA Paper No. 74-379.
54. Shaw, D., and Simitses, G. J. "Instability of Laminated Cylinders in Torsion" Journal of Applied Mechanics, Vol. 51, No.1, (1984), pp. 188-191.